Research Article

Metabolomic analysis of bone morphogenetic protein receptor type 2 mutations in human pulmonary endothelium reveals widespread metabolic reprogramming

Joshua P. Fessel[1], Rizwan Hamid[2], Bryan M. Wittmann[3], Linda J. Robinson[1], Tom Blackwell[1], Yuji Tada[4], Nobuhiro Tanabe[4], Koichiro Tatsumi[4], Anna R. Hemnes[1], and James D. West[1]

[1]Department of Medicine, Division of Allergy, Pulmonary, and Critical Care Medicine, Vanderbilt University, Nashville, Tennessee, USA, [2]Department of Pediatrics, Vanderbilt University, Nashville, Tennessee, USA, [3]Metabolon, Durham, North Carolina, USA, [4]Department of Respirology (B2), Graduate School of Medicine, Chiba University, Chiba, Japan

ABSTRACT

Pulmonary arterial hypertension (PAH) is a progressive and fatal disease of the lung vasculature for which the molecular etiologies are unclear. Specific metabolic alterations have been identified in animal models and in PAH patients, though existing data focus mainly on abnormalities of glucose homeostasis. We hypothesized that analysis of the entire metabolome in PAH would reveal multiple other metabolic changes relevant to disease pathogenesis and possible treatment. Layered transcriptomic and metabolomic analyses of human pulmonary microvascular endothelial cells (hPMVEC) expressing two different disease-causing mutations in the bone morphogenetic protein receptor type 2 (BMPR2) confirmed previously described increases in aerobic glycolysis but also uncovered significant upregulation of the pentose phosphate pathway, increases in nucleotide salvage and polyamine biosynthesis pathways, decreases in carnitine and fatty acid oxidation pathways, and major impairment of the tricarboxylic acid (TCA) cycle and failure of anaplerosis. As a proof of principle, we focused on the TCA cycle, predicting that isocitrate dehydrogenase (IDH) activity would be altered in PAH, and then demonstrating increased IDH activity not only in cultured hPMVEC expressing mutant BMPR2 but also in the serum of PAH patients. These results suggest that widespread metabolic changes are an important part of PAH pathogenesis, and that simultaneous identification and targeting of the multiple involved pathways may be a more fruitful therapeutic approach than targeting of any one individual pathway.

Key Words: pulmonary arterial hypertension, BMPR2, Warburg effect, anaplerosis, isocitrate dehydrogenase

Pulmonary arterial hypertension (PAH) is a fatal, progressive disease of the pulmonary vasculature characterized by increasing pulmonary vascular resistance that leads to right heart failure and death.[1,2] The disease exists in several forms in humans, including a heritable form caused primarily by mutations in bone morphogenetic protein receptor type 2 (BMPR2) and an idiopathic form that is clinically and in many ways molecularly indistinguishable from the inherited disease.[3-5] Despite extensive investigations in PAH patients and in a variety of animal models of PAH, the molecular mechanisms of disease pathogenesis have remained relatively obscure. Multiple converging lines of evidence point to disruption of interdependent metabolic pathways as being central to the molecular pathogenesis of PAH. In expression arrays from Bmpr2 mutant mice, nearly 50% of the significantly altered genes fall into metabolic gene ontology groups, without identification of specific metabolic pathways.[6] Several animal models of PAH

Address correspondence to:
Dr. Joshua P. Fessel
Vanderbilt University
Department of Medicine, Division of Allergy
Pulmonary, and Critical Care Medicine
1161 21st Avenue South, MCN Suite T1218
Nashville, TN 37232, USA
Email: joshua.p.fessel@vanderbilt.edu

Access this article online

Quick Response Code:	Website: www.pulmonarycirculation.org
	DOI: 10.4103/2045-8932.97606
	How to cite this article: Fessel JP, Hamid R, Wittmann BM, Robinson LJ, Blackwell T, Tada Y et al. Metabolomic analysis of bone morphogenetic protein receptor type 2 mutations in human pulmonary endothelium reveals widespread metabolic reprogramming. Pulm Circ 2012;2:201-13.

show a shift toward aerobic glycolysis, the so-called "Warburg effect" that has been identified as central to malignant transformation in a number of tumor types.[7-9] Alterations in glucose uptake and utilization, alongside changes in mitochondrial oxidative phosphorylation, have been demonstrated in the pulmonary artery endothelium from patients with PAH.[10,11] More recently, PAH patients not previously known to have diabetes or any other obvious metabolic diseases were found to have measurable increases in hemoglobin A1c compared to age- and BMI-matched controls, suggesting that whole-body glucose homeostasis is impaired in PAH.[12,13] Pulmonary hypertension associated with chronic hypoxia has been directly linked to an imbalance between glycolysis, glucose oxidation, and fatty acid oxidation.[9] Finally, therapies aimed at normalizing glucose oxidation directly (e.g., inhibitors of pyruvate dehydrogenase kinase such as dichloroacetate) or via modulation of the balance between fatty acid oxidation and glucose oxidation (e.g., partial fatty acid oxidation inhibitors such as trimetazidine or ranolazine) have shown great promise in treating PAH and have demonstrated the importance of metabolic disturbances in disease initiation and maintenance.[8,14-18] Indeed, dichloroacetate has entered Phase I trials in humans (ClinicalTrials.gov identifier NCT01083524). Though the weight of evidence suggests that metabolic reprogramming is a key feature of the molecular pathogenesis of PAH, existing data focus mainly on abnormalities of glucose homeostasis, and the full breadth and scope of the altered metabolic pathways in PAH are unknown.

We hypothesized that a broad-based metabolomic analysis of BMPR2 mutations that are known to cause PAH would reveal multiple coexisting and interdependent metabolic abnormalities beyond changes in glucose homeostasis. We quantify several hundred small molecule metabolites in native human pulmonary microvascular endothelial cells (hPMVEC) and in hPMVEC expressing one of two different disease-causing BMPR2 mutations. Organization of the significantly changed metabolites into known biochemical pathways confirms that multiple interconnected metabolic pathways are deranged in PAH. Gene expression array analysis from these same cells shows that metabolic genes represent the largest single group of significantly changed genes and support the findings from the metabolomic analyses. Using these layered metabolomic and transcriptomic analyses, we then predict alteration of the activity of a specific enzyme in the tricarboxylic acid (TCA) cycle – namely, isocitrate dehydrogenase (IDH) — as a proof of principle and demonstrate increased IDH activity in mutant hPMVEC and in the serum of patients with PAH.

MATERIALS AND METHODS

Human pulmonary microvascular endothelial cell culture

Human PMVEC were grown in culture as previously described.[19-21] Cells were maintained in Endothelial Cell Growth Medium MV from PromoCell (Heidelberg, Germany) in standard cell culture incubators (37°C, humidified, 5% CO_2) and were used at or before the 10th passage.

Generation of stably transfected hPMVEC

Cells were transfected with either empty vector (native) or vector containing BMPR2 with R332X (KD) or 2579-2580delT (CD) mutations and stably selected using G418S as previously described.[22] Endothelial character of the cells for this study was confirmed by immunohistochemistry for the von Willebrand factor and by analysis of expression arrays for a panel of endothelial markers (Figure S1A, B).

Transcriptomic analysis

Native and mutant hPMVEC were grown to 80% confluence, transitioned from G418S selection for at least 12 hours, and mRNA was isolated as described.[23] Two Affymetrix HGU133 Plus 2 arrays were run for each condition, with RNA for each array representing a pool of three independently grown plates, for a total of six arrays representing 18 biologically distinct events (three conditions × three plates × two arrays each). Results were analyzed using dChip and R statistical software. Significantly changed genes were determined using a requirement of a minimum of a 2× change, a minimum difference in expression of at least 200 arbitrary Affymetrix units, and a $P<0.01$ by a t-test for differences.

Metabolomic analysis

Full details of the methodology for the mass spectrometry-based metabolomic analyses are given in Supplemental Methods and as described previously.[24,25] Briefly, samples (N=7 for each condition) were subjected to methanol extraction, split into aliquots for analysis by ultrahigh performance liquid chromatography/mass spectrometry (UHPLC/MS) in either the positive or negative ion mode or by gas chromatography/mass spectrometry (GC/MS). Internal standards and controls for signal blank, technical replicates, and instrument performance were spiked into the samples and tracked throughout the analysis. Metabolite concentrations were determined by automated ion detection, manual visual curation, and were analyzed in-line using software developed by Metabolon.[26] Significance was set at $P<0.05$ by Welch's two-sample t-test with correction for multiple comparisons using q-values.[27]

$NADP^+$-dependent IDH activity assays

IDH activity assays were performed using the BioVision Isocitrate Dehydrogenase Activity Assay Kit (Mountain

View, Calif.) according to the manufacturer's instructions. For hPMVEC, cells were grown in 6-well plates to 50—60% confluence to yield approximately 500,000 cells per well, harvested, and lysed directly in the assay buffer. Aliquots were used for the IDH activity assay and for protein concentration determination by Pierce BCA assay. For serum, samples were used as undiluted 50 µl aliquots and assayed for IDH activity according to the instructions.

Human subjects

All patients and normal volunteers provided written informed consent to participate in research protocols approved by the institutional review boards of all participating institutions (IRB protocol number 9401). Blood was drawn by standard venipuncture, centrifuged to collect serum, and serum was stored at −80°C until analysis.

Statistical analyses

Analyses were performed using R statistical software and using GraphPad Prism. Welch's t-test or two-way ANOVA were used for tests of statistical significance. Box-and-whisker plots represent 25th—75th percentiles with the box, the median with the center line, and Tukey whiskers representing 1.5 times the interquartile range. Scatter plots show individual data points with mean±SEM depicted. For most analyses, significance was set at $P<0.05$, with $P<0.01$ being used as the significance threshold for RNA expression microarray analysis.

RESULTS

BMPR2 mutations resulted in widespread changes in endothelial cell gene expression that organized into specific pathways

We sought to compare expression arrays from native hPMVEC to those from hPMVEC expressing one of two mutant BMPR2 constructs, and to organize the significantly different genes into functional pathways. Human pulmonary microvascular endothelial cells were stably transfected with either R332X mutation in the kinase domain (KD) or a 2579-2580delT mutation in the cytoplasmic tail domain (CD). The CD mutation has been previously shown to dysregulate BMPR2 interaction with and signaling through LIMK-1, c-Src, and Tctex-1;[28-31] the KD mutation also includes dysregulated signaling through the canonical Smad pathway.[32]

Using a requirement of a minimum of twofold change, a minimum difference in expression of at least 200 arbitrary Affymetrix units, and a $P<0.01$ by t-test for difference, we found 687 probe sets representing 507 unique Entrez IDs, with common changes between both BMPR2 mutants and native hPMVEC, with a false discovery rate (FDR) of zero (determined by scrambling group identifiers). These data have been deposited in GEO, accession number pending , and a full list of the 507 genes is provided in Supplemental Dataset S1. Distribution of gene ontology groups was nearly identical to our previously published expression arrays interrogating PMVEC isolated from our $Bmpr2^{R899X}$ and $Bmpr2^{delx4+}$ mouse models.[6,33,34] These included genes involved in apoptosis, proliferation, stimulus response, cytoskeletal organization, and development (Fig. 1). Roughly 40% of the genes changed (216/507) were related to small molecule metabolism. Heterologous expression of BMPR2 mutations resulted in broad changes in TCA cycle, glycolysis, hypoxia-inducible factor (HIF) responsive metabolic elements, and carnitine, fatty acid, and glutamate metabolism compared to expression of native BMPR2. Relatively unaffected pathways include glycan synthesis and metabolism, vitamin/cofactor metabolism (with the exception of folate and single-carbon metabolism), and xenobiotic metabolism. Thus, the affected pathways showed a degree of specificity as opposed to nonspecific whole metabolome dysfunction.

Metabolomic analysis of BMPR2 mutant endothelial cells showed significant alteration of multiple interdependent metabolic pathways

To determine the whole metabolome consequences of disease-causing BMPR2 mutation in endothelial cells, we undertook a simultaneous multiplexed mass spectrometric quantification of several hundred small molecule metabolites in CD and KD mutant hPMVEC and compared these mutations to the native hPMVEC. In this analysis, 267 small molecule metabolites were confidently identified in seven biological replicates for each condition described above (native, CD, and KD, Figure S2). Significantly changed biochemicals from the native condition were identified as those biochemicals with a P-value <0.05 based upon Welch's two-sample t-test, which had a maximum FDR of 3.2% based upon q-values[27] for that set of biochemicals with P-values <0.05. The full dataset is provided in Supplemental Dataset S2. Compared to the native hPMVEC, the CD mutants showed significant changes in 65% of the metabolites quantified (172/267, with 87 increased and 85 decreased) and the KD mutants showed significant changes in 37% of the metabolites (99/267, with 61 increased and 38 decreased). This represented confident identification of approximately 11% of the database of named compounds available in this analysis, with the CD mutants showing significant changes in the levels of approximately 7% of the total compounds in the database. For the KD mutants, a further 14% (38 metabolites) approached statistical significance ($0.05<P<0.10$ by Welch's two-sample t-test), though these were not included in the analyses discussed below.

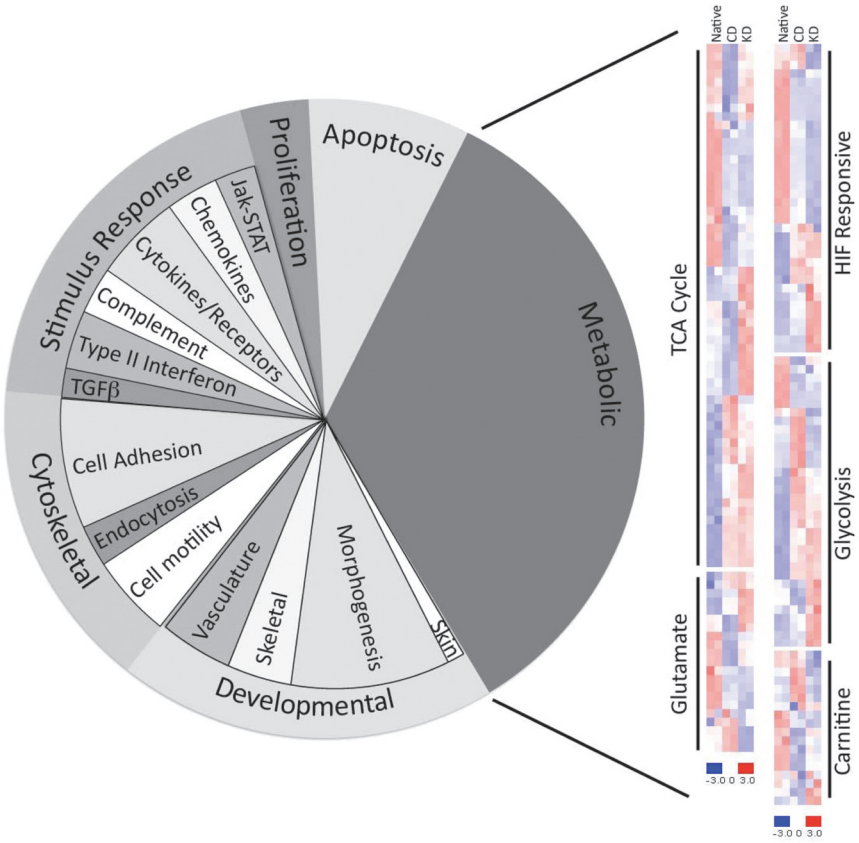

Figure 1: Transcriptomic analysis of human pulmonary microvascular endothelial cells expressing one of two dominant negative BMPR2 mutant constructs. The pie chart depicts the pathways represented by the 507 genes showing significantly altered expression in the CD and KD mutant hPMVEC compared to the native hPMVEC. The largest single major ontology group was metabolic genes, and the heatmap at the right of the figure shows changes in individual genes within this larger group broken down by subsets, with red indicating increased expression and blue denoting decreased expression.

Increased pentose phosphate pathway metabolites and polyamine biosynthesis indicate increased proliferation in BMPR2 mutant endothelial cells

Intermediates in the pentose phosphate pathway for BMPR2 mutant hPMVEC along with changes in the expression of the corresponding genes compared to native hPMVEC are shown (Fig. 2). The pentose phosphate pathway interfaces with multiple other metabolic pathways, including the glycolytic pathway and NADPH synthetic pathways, in addition to providing 5-carbon sugars for nucleotide synthesis. The enzyme primarily responsible for synthesis of NADPH in the pentose phosphate pathway, glucose-6-phosphate dehydrogenase, exhibited significantly reduced expression in both the CD and KD mutants. The upregulation of the pentose phosphate pathway in the BMPR2 mutant hPMVEC thus was apparently driven by upregulation from ribose-5-phosphate isomerase downstream that overcame decreases in glucose-6-phosphate dehydrogenase expression and that directly related to increased nucleotide synthesis and salvage. The significantly increased levels of purine and pyrimidine nucleosides downstream from both mutations further supported this conclusion. Finally, intermediates in the terminal portion of the polyamine synthesis pathway in the CD and KD mutants were increased preferentially over urea cycle intermediates (Figure S3), further supporting the increased cell proliferation previously observed for these specific mutations.[6]

Multiple energy metabolism pathways were disrupted in BMPR2 mutant endothelium

Several groups have previously shown an increase in aerobic glycolysis (the "Warburg effect") in PAH,[7-9,35] and increased glucose uptake has been demonstrated in the lungs of PAH patients by positron emission tomography.[10] In this whole metabolome analysis, glycolysis showed significant upregulation as a consequence of BMPR2 mutation, though this was not to the same extent for both mutations (Fig. 3). Glycolytic metabolites were significantly increased in the CD mutants for all of the pathway intermediates down to pyruvate, whereas the KD mutants showed statistically significant increases or trends in increases only for the metabolites earlier in the glycolytic pathway. Consistent with global activation of the glycolytic pathway, expression of the majority of the genes for glycolytic enzymes was increased, including genes coding for glucose uptake transporters. The genes for two of the three regulated enzymes in the pathway, hexokinase, and phosphofructokinase, showed decreased expression in arrays from the BMPR2 mutant hPMVEC, though the third regulated enzyme, pyruvate kinase, showed increased expression for at least one isoform.

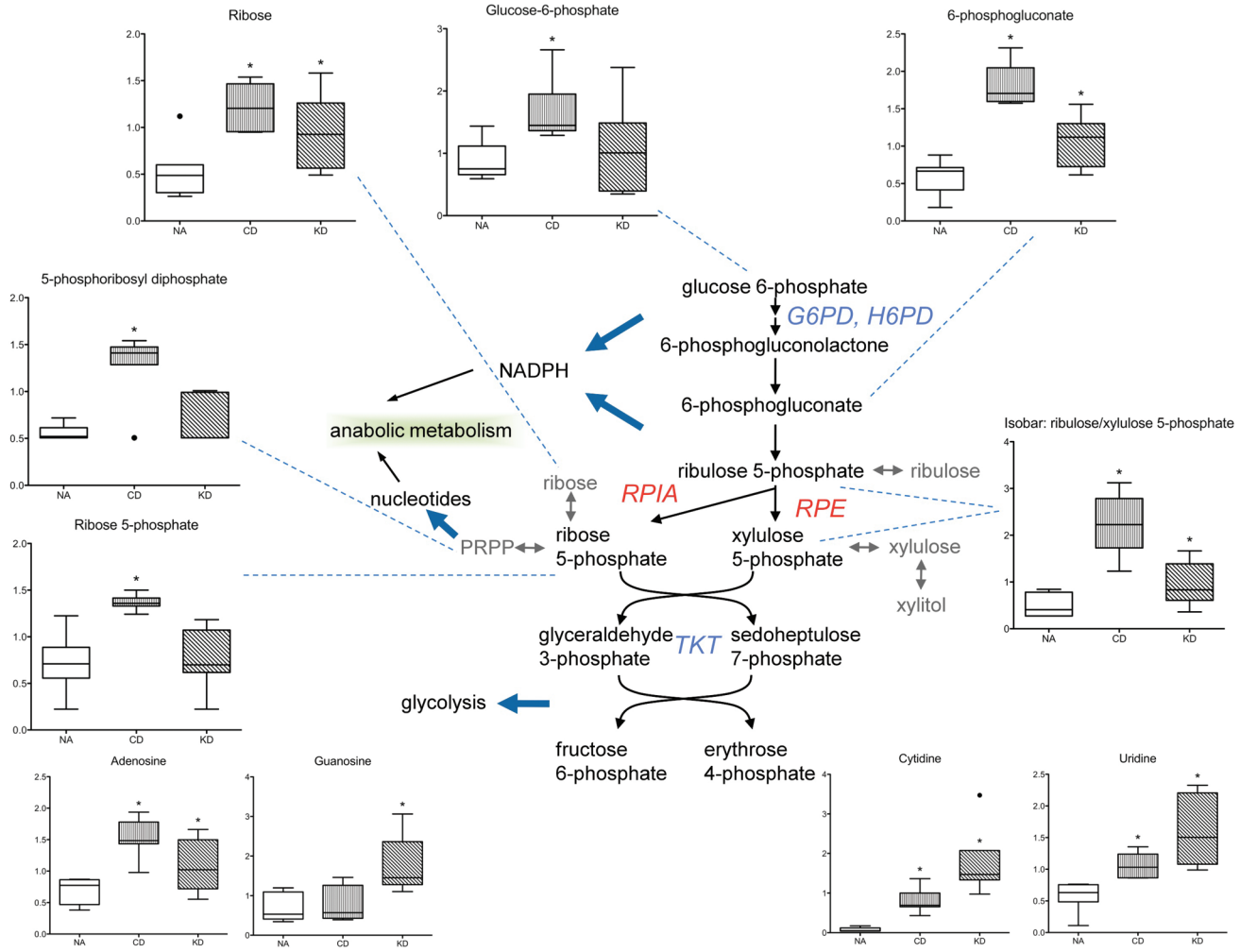

Figure 2: Intermediates in the pentose phosphate pathway specific to nucleotide synthesis are increased in BMPR2 mutant hPMVEC. Major intermediates in the pentose phosphate pathway are shown. In all graphs, native hPMVEC are in white boxes, CD hPMVEC in vertical hatched boxes, and KD hPMVEC in diagonal hatched boxes. Quantities are in arbitrary units specific to the internal standards for each quantified metabolite and normalized to protein concentration. N = 7 for each box, with whiskers indicating Tukey whiskers and extreme data points indicated by filled circles. *P<0.05 compared to native. Genes coding for the enzymes that catalyze particular steps in the pathway are indicated by their Entrez Gene names, with red indicating significantly increased expression in the transcriptomic analysis and blue indicating significantly decreased expression. The four graphs at the bottom of the figure show quantitation of purine and pyrimidine nucleosides. G6PD, glucose-6-phosphate dehydrogenase; H6PD, hexose-6-phosphate dehydrogenase; RPIA, ribose-5-phosphate isomerase A; RPE, ribulose-5-phosphate-3-epimerase; TKT, transketolase.

The interplay between fatty acid oxidation and glucose utilization has been shown to play an important role in pulmonary hypertension related to chronic hypoxia and in right ventricular hypertrophy and failure induced by pressure overload in a pulmonary artery banding model,[9,18] but this has not been explored in pulmonary arterial hypertension specifically. We thus sought evidence for alterations in the major pathways for fatty acid oxidative metabolism in the context of disease-causing BMPR2 mutations. We found that carnitine and its downstream acyl metabolites were significantly reduced in the CD and KD mutant hPMVEC compared to the native endothelial cells (Fig. 4). Decreased levels of carnitine itself as well as glycine (a by-product of carnitine synthesis) suggested decreased synthesis of carnitine itself. Levels of palmitoylcarnitine, isobutyrylcarnitine, and propionylcarnitine were also significantly decreased. Decreased expression of many of the key genes involved in carnitine/acylcarnitine metabolism and trafficking was also observed, including the two major carnitine palmitoyltransferase genes and one of the major carnitine/acylcarnitine translocases. We also found significantly decreased expression of a number of the acyl-CoA dehydrogenase genes involved in fatty acid oxidation.

Activity of the tricarboxylic acid (TCA) cycle has been shown to be reduced in a variety of different types of cancer, and this has been proposed to be a central advantage exploited by cancer cells, allowing for diversion of TCA cycle intermediates toward macromolecule synthesis while relying on other energy-generating pathways such as

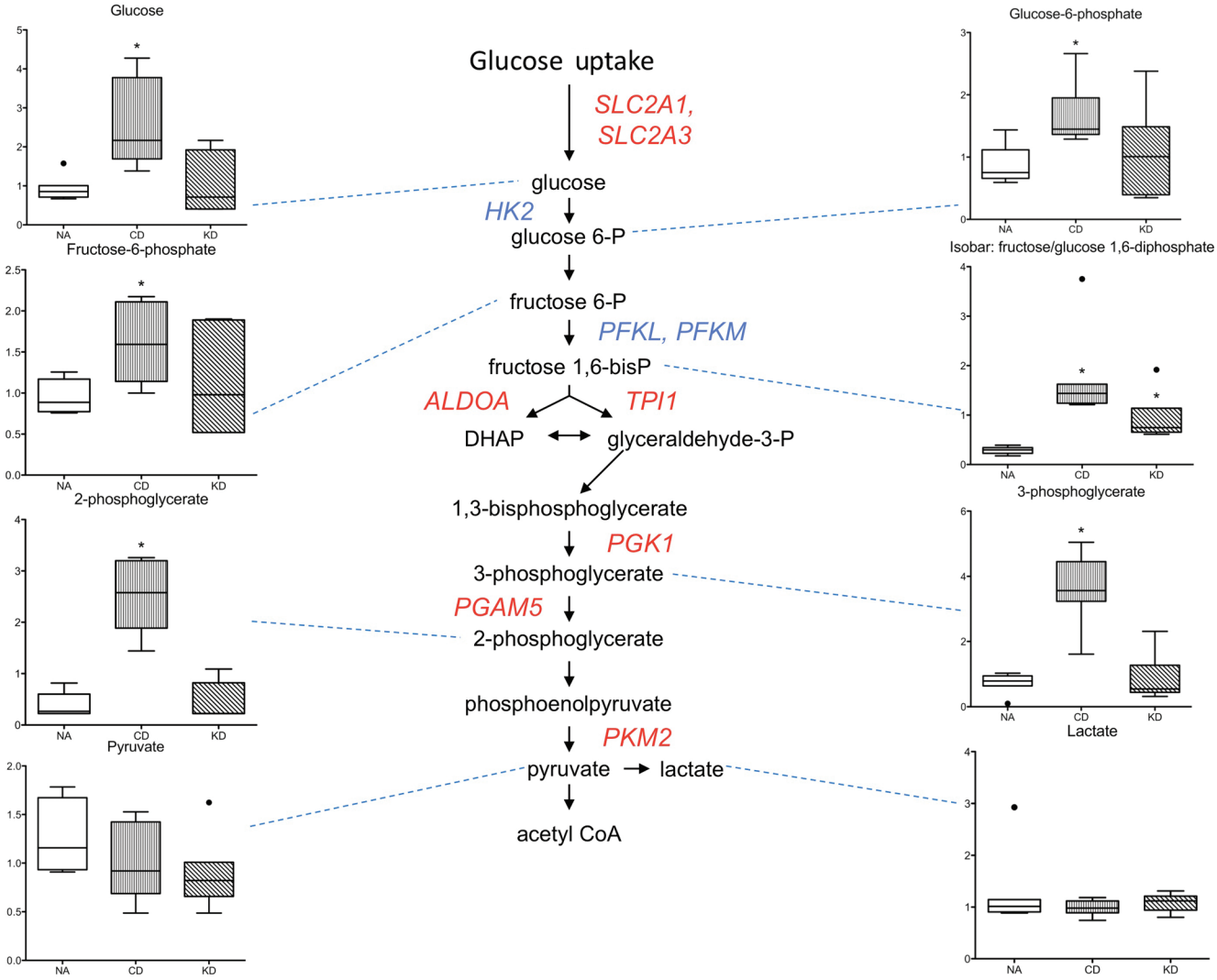

Figure 3: Glycolysis is significantly upregulated in BMPR2 mutant hPMVEC, particularly in cytoplasmic tail domain mutants. The classical glycolysis pathway intermediates are shown. In all graphs, native hPMVEC are in white boxes, CD hPMVEC in vertical hatched boxes, and KD hPMVEC in diagonal hatched boxes. Quantities are in arbitrary units specific to the internal standards for each quantified metabolite and normalized to protein concentration. N = 7 for each box, with whiskers indicating Tukey whiskers and extreme data points indicated by filled circles. **P*<0.05 compared to native. Genes coding for the enzymes that catalyze particular steps in the pathway are indicated by their Entrez Gene names, with red indicating significantly increased expression in the transcriptomic analysis and blue indicating significantly decreased expression. *SLC2A1* and *SLC2A3*, solute carrier family 2 (facilitated glucose transporter), members 1 and 3; *HK2*, hexokinase 2; *PFKL* and *PFKM*, phosphofructokinase, liver and muscle isoforms; *ALDOA*, aldolase A; *TPI1*, triosephosphate isomerase 1; *PGK1*, phosphoglycerate kinase 1; *PGAM5*, phosphoglycerate mutase 5; *PKM2*, pyruvate kinase, muscle.

glycolysis.[36-38] Although a number of the metabolic features of cancer cells have been observed in PAH, defects in the TCA cycle have not been extensively described. In hPMVEC expressing BMPR2 mutations, there were extensive metabolic defects in the TCA cycle indicating overall decreased activity of the cycle downstream from citrate (Fig. 5). In particular, significant decreases in succinate, fumarate, and malate were present in the CD mutants, whereas much more mild nonsignificant decreases in the mean concentrations of succinate and malate were observed for the KD mutants. In both mutants, concentrations of citrate were significantly increased, and concentrations of pyruvate and lactate were equivalent to the native hPMVEC, suggesting that the defect in the TCA cycle occurred distal to citrate. Moreover, this suggested that alternative catabolic pathways (e.g., fatty acid oxidation, peptide/amino acid catabolism) feeding into the TCA cycle were insufficient to support concentrations of succinate, fumarate, and malate, particularly in the CD mutants. The balance of TCA cycle intermediates is normally maintained by the complementary processes of anaplerosis and cataplerosis. Broadly defined, anaplerosis refers to the addition of 4- and 5-carbon intermediates into the TCA cycle (e.g., oxaloacetate, alpha-ketoglutarate, and succinyl-CoA) using pyruvate, aspartate, glutamate, or fatty acids as substrates, to support mitochondrial respiration and to replenish TCA cycle intermediates diverted to biosynthesis. Cataplerosis refers to the removal of these same TCA cycle intermediates

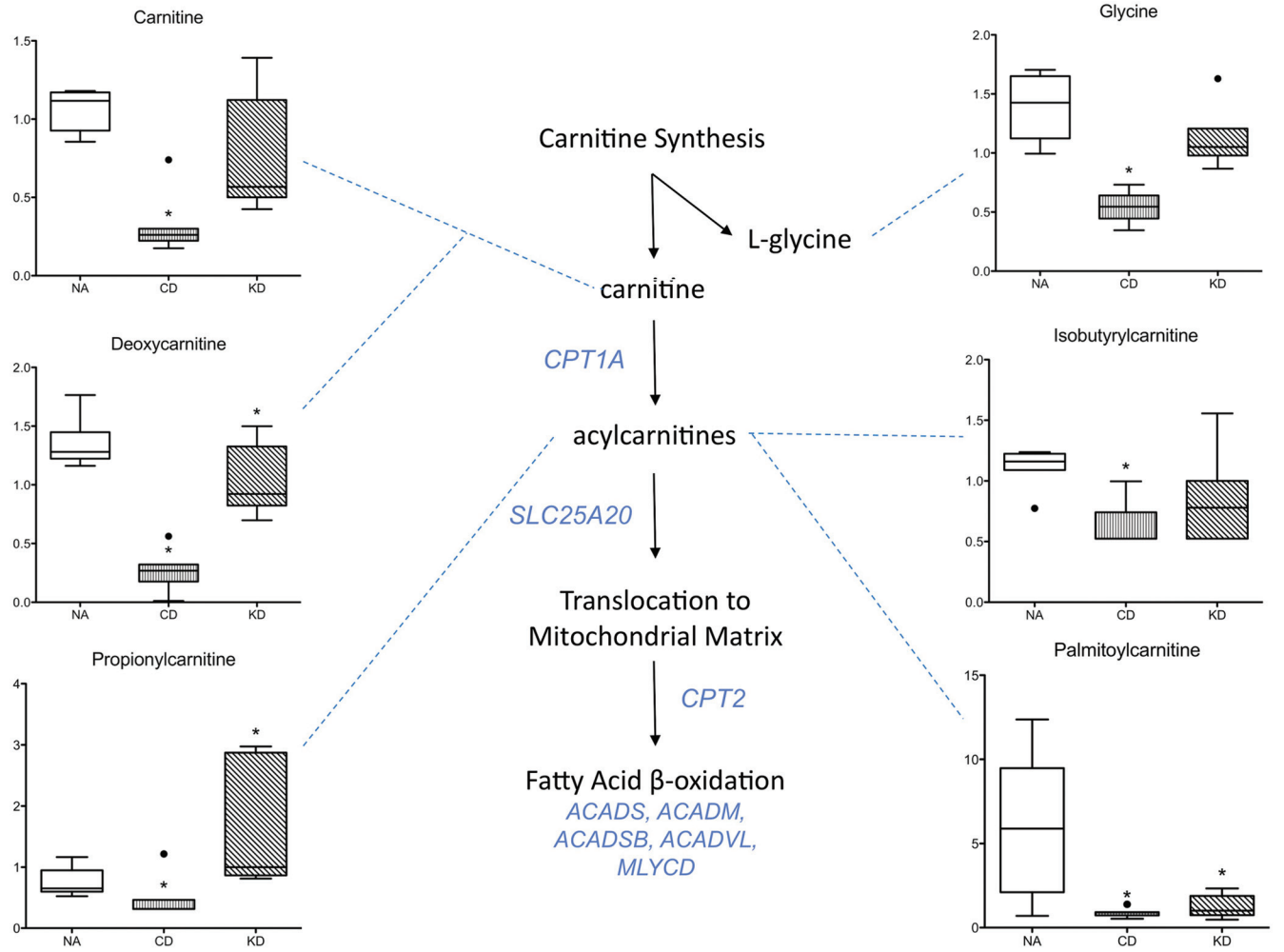

Figure 4: Carnitine metabolism and fatty acid oxidation are significantly depressed in BMPR2 mutant hPMVEC. Multiple carnitine metabolites and their flow into fatty acid oxidation are shown. Intermediates for which significant differences in one or both mutant conditions were detected are shown. In all graphs, native hPMVEC are in white boxes, CD hPMVEC in vertical hatched boxes, and KD hPMVEC in diagonal hatched boxes. Quantities are in arbitrary units specific to the internal standards for each quantified metabolite and normalized to protein concentration. N = 7 for each box, with whiskers indicating Tukey whiskers and extreme data points indicated by filled circles. *P<0.05 compared to native. Genes coding for the enzymes that catalyze particular steps in the pathway are indicated by their Entrez Gene names, with red indicating significantly increased expression in the transcriptomic analysis and blue indicating significantly decreased expression. CPT1A and CPT2, carnitine palmitoyltransferase isoforms 1A and 2; SLC25A20, carnitine/acylcarnitine translocase; ACADS, ACADM, ACADSB, and ACADVL, acyl-CoA dehydrogenases – short chain, medium chain, short/branched chain, and very long chain; MLYCD, malonyl-CoA decarboxylase.

to support biosynthetic processes such as gluconeogenesis, glyceroneogenesis, and fatty acid synthesis.[39]

Two key specific anaplerotic pathways are the conversion of glutamine to glutamate and then to alpha-ketoglutarate, and the conversion of aspartate to oxaloacetate.[40] Levels of these specific amino acids were quantified and found to be significantly reduced in the CD mutant hPMVEC compared to native cells (Fig. 6). By contrast, the KD mutants showed increased levels of glutamine and glutamate, which likely contributed to the more modest reductions of TCA cycle intermediates in these cells, as there was more glutamine and glutamate available for the anaplerotic synthesis of alpha-ketoglutarate. The differences between the CD and KD mutants may be at least in part attributable to differences in the synthesis of N-acetylaspartylglutamate (NAAG). The CD mutants showed increased expression of NAAG synthetase and increased concentrations of NAAG, whereas the KD mutants showed decreased expression of NAAG synthetase and a subsequently lower level of NAAG compared to the CD mutants. It thus is likely that, in the CD mutants, much of the glutamate and aspartate that might otherwise have been used to feed into the TCA cycle was instead being used for the synthesis of NAAG. This was not the case in the KD mutants. Both mutations appeared to drive an overall increase in peptide and amino acid catabolism, as both mutants showed significant increases

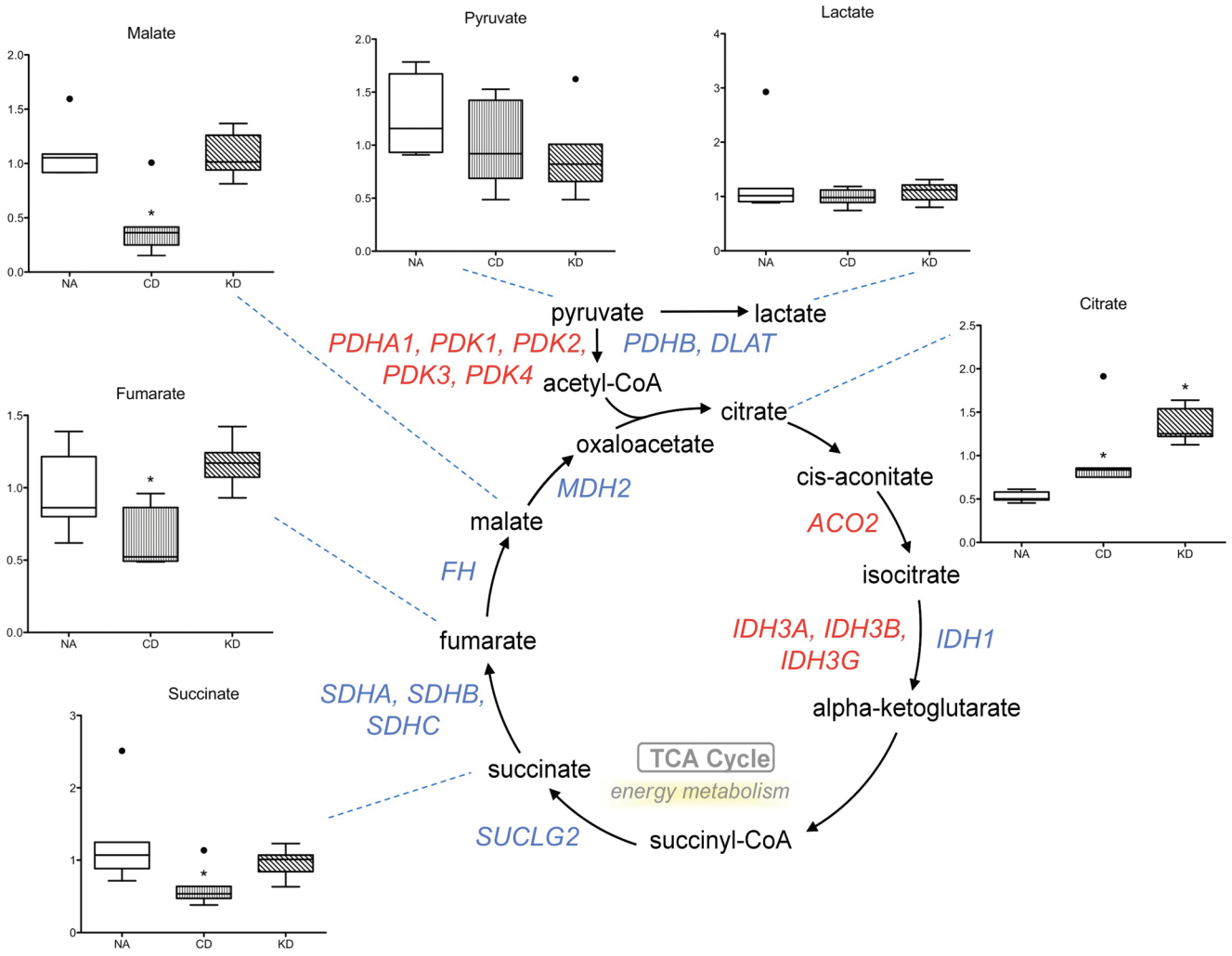

Figure 5: TCA cycle intermediates are significantly decreased in BMPR2 mutant hPMVEC, particularly in CD mutants. The TCA cycle and its major intermediates are shown. In all graphs, native hPMVEC are in white boxes, CD hPMVEC in vertical hatched boxes, and KD hPMVEC in diagonal hatched boxes. Quantities are in arbitrary units specific to the internal standards for each quantified metabolite and normalized to protein concentration. N = 7 for each box, with whiskers indicating Tukey whiskers and extreme data points indicated by filled circles. *$P < 0.05$ compared to native. Genes coding for the enzymes that catalyze particular steps in the pathway are indicated by their Entrez Gene names, with red indicating significantly increased expression in the transcriptomic analysis and blue indicating significantly decreased expression. *PDK1-4*, pyruvate dehydrogenase kinase 1-4; *PDHA1*, pyruvate dehydrogenase (lipoamide) alpha 1; *PDHB*, pyruvate dehydrogenase E1 component, beta subunit; *DLAT*, dihydrolipoamide S-acetyltransferase; *ACO2*, aconitase 2; *IDH3A/B/G*, isocitrate dehydrogenase 3 (NAD^+) alpha, beta, and gamma subunits; *IDH1*, isocitrate dehydrogenase 1 ($NADP^+$); *SUCLG2*, succinate-CoA ligase, GDP-forming, beta subunit; *SDHA/B/C*, succinate dehydrogenase complex subunits A (flavoprotein), B (iron-sulfur), and C (15kDa integral membrane protein); *FH*, fumarate hydratase; *MDH2*, malate dehydrogenase 2.

in the concentrations of dipeptides (Figure S4), though this was more pronounced in the CD mutants. In addition, anaplerosis via branched chain amino acid metabolism appeared to be more significantly impaired in the CD mutants compared to the KD mutants, as evidenced by more significant decreases in isobutyrylcarnitine and propionylcarnitine, metabolites that participate in branched chain amino acid metabolism as well as fatty acid metabolism. The CD mutants exhibited a major failure of anaplerosis on multiple levels that was much more mild in the KD mutants, and thus must rely on multiple "salvage" pathways of peptide/amino acid catabolism.

Predicted differences in IDH1/2 activity were present in mutant hPMVEC and in human PAH patients

We chose to examine the TCA cycle in more detail, as this is a major point of integration of multiple pathways involved in energy production as well as biosynthesis and so might better reflect the summation of alterations in these many different pathways. On closer inspection of the transcriptomic and metabolomic data relevant to the TCA cycle, there was a clear functional change in the BMPR2 mutants compared to the wild-type endothelial cells that occurred somewhere between citrate and succinate. The two most likely enzymatic candidates were aconitase and

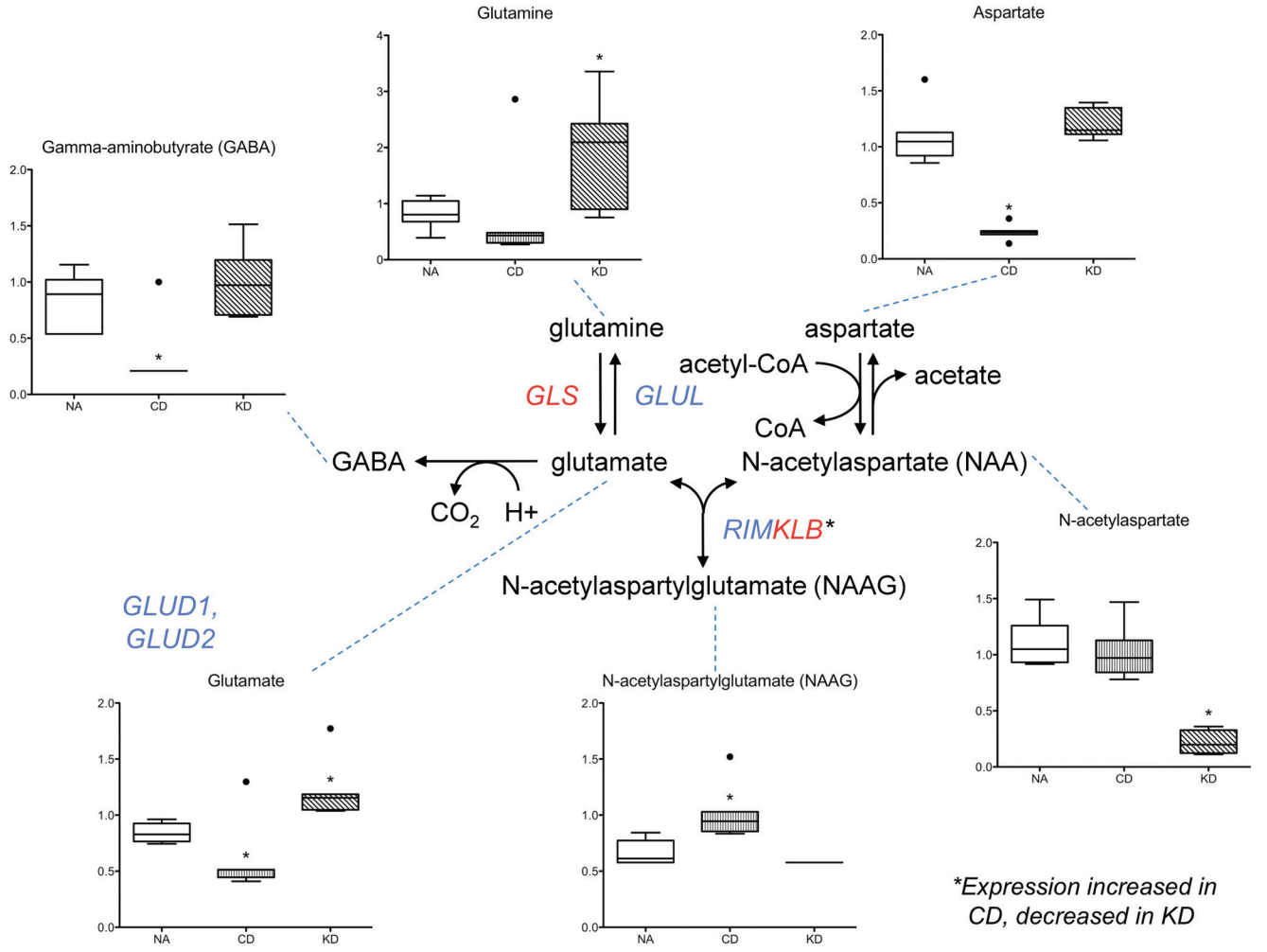

Figure 6: Glutamine/glutamate and aspartate metabolism, two major anaplerotic pathways, are significantly reduced in CD mutant hPMVEC. Intermediates for which significant differences in one or both mutant conditions were detected are shown. In all graphs, native hPMVEC are in white boxes, CD hPMVEC in vertical hatched boxes, and KD hPMVEC in diagonal hatched boxes. Quantities are in arbitrary units specific to the internal standards for each quantified metabolite and normalized to protein concentration. N = 7 for each box, with whiskers indicating Tukey whiskers and extreme data points indicated by filled circles. *P<0.05 compared to native. Genes coding for the enzymes that catalyze particular steps in the pathway are indicated by their Entrez Gene names, with red indicating significantly increased expression in the transcriptomic analysis and blue indicating significantly decreased expression. GLUD1 and GLUD2, glutamate dehydrogenase 1 and 2; GLS, glutaminase; GLUL, glutamate-ammonia ligase; RIMKLB, N-acetylaspartylglutamate synthetase B.

isocitrate dehydrogenase (IDH). Of these two enzymes, aconitase has been shown to be inactivated by oxidative stress,[41] and oxidative stress is known to be increased in the context of BMPR2 mutations.[22] To remove this as a confounding factor, we chose to examine IDH activity. While NAD^+-dependent IDH activity (corresponding to the IDH3 isoform) did not differ between wild-type and BMPR2 mutant endothelial cells, $NADP^+$-dependent IDH activity (corresponding to IDH isoforms 1 and 2, hereafter IDH1/2) was significantly increased in BMPR2 mutant endothelial cells (Fig. 7A). We then sought to determine if these findings were applicable to patients with PAH. We quantified IDH1/2 activity in serum from controls, from patients with heritable PAH known to have BMPR2 mutations, and from two pooled cohorts of patients with IPAH (one from the United States and one from Japan). Serum IDH1/2 activity was significantly increased in both HPAH and IPAH patients compared to controls (Fig. 7B). The variability in IDH1/2 activity observed in the PAH patients likely does reflect variability in disease activity, at least in part. We separated the PAH patients for whom data were available into two groups based upon the presence or absence of any prostanoid therapy (intravenous, subcutaneous, or inhaled prostacyclin receptor agonist) and analyzed serum IDH1/2 activity (Figure S5). Though only approaching statistical significance (P=0.1 by Welch's t-test), the mean serum IDH1/2 activity for the prostanoid treated group of PAH patients clearly trended toward being higher than for the nontreated group. As prostanoid therapy is only initiated in more severe disease, the higher serum IDH activity may well be a reflection of disease severity.

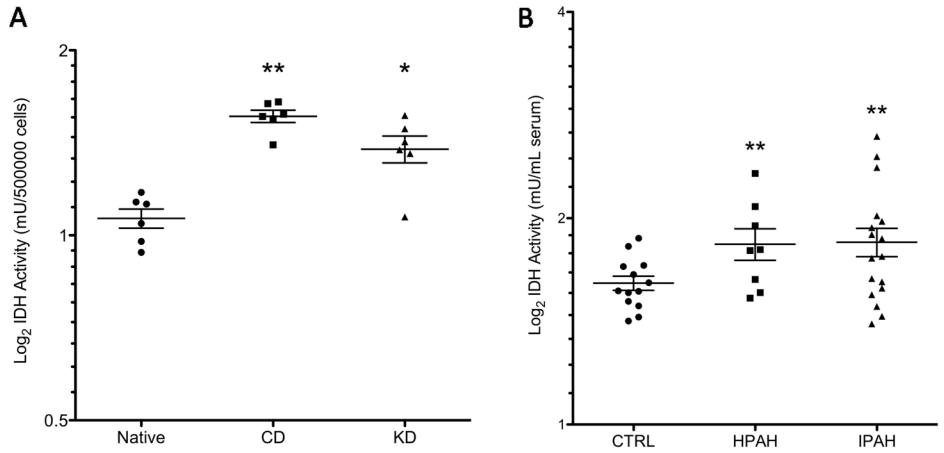

Figure 7: IDH1/2 activity is increased in mutant hPMVEC and in serum from patients with pulmonary arterial hypertension. **(A)** Compared to native hPMVEC (1.07±0.04 mU/5×10^5 cells), the CD and KD mutant-expressing hPMVEC both show significantly increased NADP$^+$-dependent IDH activity in cell lysates (1.56±0.04 and 1.38 +/ 0.07 mU/5×10^5 cells, respectively). N=6 for each group, mean±SEM indicated, $P<0.0001$ by one-way ANOVA, $^{**}P<0.0001$ vs. native, $^{*}P<0.003$ vs. native. **(B)** NADP$^+$-dependent IDH activity in the serum from patients with heritable PAH (N=8, 1.83±0.1 mU/mL) and idiopathic PAH (N=17, 1.85±0.09 mU/mL) was significantly increased compared to serum from normal control individuals (N=13, 1.61±0.04 mU/mL), mean±SEM indicated, $^{**}P<0.03$ vs. control by Welch's t-test.

DISCUSSION

We present here a whole metabolome analysis of the effects of BMPR2 mutations known to cause pulmonary arterial hypertension. We have constructed an integrated picture of the complex and interdependent metabolic changes that occur downstream from BMPR2 mutations in human pulmonary microvascular endothelial cells, and this integrated view has demonstrated more widespread metabolic defects in PAH than have been previously known. The shift toward aerobic glycolysis that is typified by the Warburg effect in PAH has been known for some time.[7] More recently, the interplay between fatty acid oxidation and control of glycolysis versus glucose oxidation (typified by the Randle cycle) has been demonstrated to be important in hypoxic pulmonary hypertension.[9,42] In addition to confirming these previously identified metabolic defects in PAH, we have identified significant alterations in the TCA cycle and at least some of the pathways that interact with it.

Our analysis reveals a profound failure of anaplerosis present downstream from BMPR2 mutations that has been largely unexplored as a mechanism of disease pathogenesis in PAH. TCA cycle intermediates are depleted through what appears to be a combination of decreased activity of the cycle itself plus abnormal shunting of intermediates from other pathways (e.g., glutamate, glutamine, aspartate, and branched chain amino acids) that could otherwise be used to replenish the intermediates of the TCA cycle. This implies that the metabolic defects in PAH cannot be simply summed up under the umbrella of Warburg metabolism.[35,43] It is possible that diversion of TCA cycle intermediates for biosynthesis and reliance on aerobic glycolysis is actually a feature of decreased BMP signaling, as would be seen in settings of tissue remodeling and repair, for example. However, these would be settings of temporary loss or reduction of BMP signaling, and what might be adaptive cataplerosis in the short-term becomes pathogenic in the setting of permanently decreased BMP signaling due to mutation. More importantly, the therapeutic implication is that it is very likely that most or all of the errant pathways will need to be targeted to expect a significant therapeutic impact, and current investigational therapies address only certain dysfunctional pathways that largely do not address the failure of anaplerosis.

To demonstrate further the utility of our combined metabolomic and transcriptomic analysis, we chose to quantify NADP$^+$-dependent IDH activity. We predicted that this enzymatic activity would be altered in PAH and then demonstrated the accuracy of that prediction in both cultured cells and in patients with PAH. Alterations in IDH activity have not been previously described in PAH; however, multiple conceptual links between PAH and cancer have been proposed, and there is a growing body of literature linking altered IDH activity in a causative way to at least certain types of cancer,[24,44-47] so the identification of altered IDH1/2 activity in PAH may in fact be directly related to disease pathogenesis.

A second possibility is that the anaplerotic failure and increased IDH1/2 activities in PAH are driving forces for HIF activation that underlies PAH,[15,48] which then perpetuates increased aerobic glycolysis, apoptosis resistance, and decreased mitochondrial number.[11] HIF can be activated by decreased alpha-ketoglutarate and increased citrate concentrations, both of which activate

HIF by decreasing the efficiency of prolyl hydroxylase.[49] Under hypoxic conditions, activation of HIF has very recently been shown to increase IDH2-mediated conversion of glutamine-derived alpha-ketoglutarate to citrate.[50] The resultant hypothesized increase in citrate and decrease in alpha-ketoglutarate brought about by increased IDH2 activity would thus be predicted to further drive HIF activation, setting up something of a vicious cycle. Our data show significant changes in the expression of HIF responsive genes in BMPR2 mutant hPMVEC. Alternatively, HIF activation can be driven by increased oxidative stress and decreased antioxidant defenses, as is seen with epigenetic inactivation of SOD2,[51] and this may be the upstream event that drives IDH activation. HIF activation can drive metabolic reprogramming that leads to increased IDH activity,[50] and IDH may be upregulated in response to oxidative stress to serve as a source of NADPH that is used to maintain reduced glutathione pools intracellularly.[52]

More importantly, IDH activity appears to track with disease activity, as patients with more severe disease (i.e., those treated with a prostacyclin agonist) trend toward higher serum IDH activity. The fact that those patients with disease severe enough to warrant prostanoid therapy still exhibit increased serum IDH activity after the initiation of therapy suggests that our most efficacious class of drugs for PAH still does not correct all of the underlying metabolic defects in PAH and highlights the need for therapies that arise from a deeper understanding of the molecular pathogenesis of PAH. Further investigations are needed to determine if the increased IDH activity described in PAH in this study is truly pathogenic, adaptive, or epiphenomenon.

This type of investigation is not without limitations. The pulmonary endothelial cell clearly plays an important role in the pathogenesis of PAH, but many other cell types, including smooth muscle cells,[53] lung mesenchymal stem cells,[54] and resident immune cells[55] all likely contribute to disease development. It is not possible in most cases in this study to determine what changes are truly causative of disease and which are consequences of the disease, although examination of cells in culture minimizes this problem to some degree.[23] While identification of putative molecular targets is possible and is greatly enhanced by this type of layered analysis, each target must be further validated independently and placed into a context. Still, this study has permitted the identification of previously unrecognized pathways that likely directly contribute to the development of PAH; the identification of promising new biomarkers, of which IDH1/2 activity is but one, to guide diagnosis and therapeutic evaluation; and the recognition of the importance of defining and simultaneously targeting the multiple affected metabolic pathways in future therapeutic development. We hypothesize that this approach would be similarly fruitful in many other complex diseases.

APPENDIX

Supplemental Methods

Metabolomic Analysis: Native and mutant hPMVEC were grown to 80% confluence (yielding approximately 1-3 $\times 10^7$ cells per sample), transitioned from G418 sulfate selection to complete media without antibiotic for at least 12 hours, and washed with phosphate-buffered saline and trypsinized to harvest cells. Cells were pelleted, the supernatant removed, and the dry pellet snap frozen in liquid nitrogen and stored at -80C until analysis. The non-targeted metabolic profiling platform employed for this analysis combined three independent platforms: ultrahigh performance liquid chromatography/tandem mass spectrometry (UHPLC/MS/MS^2) optimized for basic species, UHPLC/MS/MS^2 optimized for acidic species, and gas chromatography/mass spectrometry (GC/MS). Samples were processed essentially as described previously.[1,2] For each sample, 100L was used for analyses. Using an automated liquid handler (Hamilton LabStar, Salt Lake City, UT), protein was precipitated from the homogenate with methanol that contained four standards to report on extraction efficiency. The resulting supernatant was split into equal aliquots for analysis on the three platforms. Aliquots, dried under nitrogen and vacuum-desiccated, were subsequently either reconstituted in 50L 0.1% formic acid in water (acidic conditions) or in 50L 6.5mM ammonium bicarbonate in water, pH 8 (basic conditions) for the two UHPLC/MS/MS^2 analyses or derivatized to a final volume of 50L for GC/MS analysis using equal parts bistrimethyl-silyl-trifluoroacetamide and solvent mixture acetonitrile:dichloromethane:cyclohexane (5:4:1) with 5% triethylamine at 60°C for one hour. In addition, three types of controls were analyzed in concert with the experimental samples: aliquots of a well-characterized human plasma pool served as technical replicates throughout the data set, extracted water samples served as process blanks, and a cocktail of standards spiked into every analyzed sample allowed instrument performance monitoring. Experimental samples and controls were randomized across platform run days.

For UHLC/MS/MS^2 analysis, aliquots were separated using a Waters Acquity UPLC (Waters, Millford, MA) and analyzed using an LTQ mass spectrometer (Thermo Fisher Scientific, Inc., Waltham, MA) which consisted of an electrospray ionization (ESI) source and linear ion-trap (LIT) mass analyzer. The MS instrument scanned 99-1000 m/z and alternated between MS and MS^2 scans

using dynamic exclusion with approximately 6 scans per second. Derivatized samples for GC/MS were separated on a 5% phenyldimethyl silicone column with helium as the carrier gas and a temperature ramp from 60°C to 340°C and then analyzed on a Thermo-Finnigan Trace DSQ MS (Thermo Fisher Scientific, Inc.) operated at unit mass resolving power with electron impact ionization and a 50-750 atomic mass unit scan range.

Metabolites were identified by automated comparison of the ion features in the experimental samples to a reference library of chemical standard entries that included retention time, molecular weight (m/z), preferred adducts, and in-source fragments as well as associated MS spectra, and were curated by visual inspection for quality control using software developed at Metabolon.[3]

For statistical analyses and data display purposes, any missing values were assumed to be below the limits of detection and these values were imputed with the compound minimum (minimum value imputation). Statistical analysis of log-transformed data was performed using "R" (http://cran.r-project.org/). Welch's t-tests were performed to compare data between experimental groups. A p-value of < 0.05 was considered statistically significant and multiple comparisons were accounted for by estimating the false discovery rate (FDR) using q-values.[4]

REFERENCES

1. Runo JR, Loyd JE. Primary pulmonary hypertension. Lancet 2003;361: 1533-44.
2. Agarwal R, Gomberg-Maitland M. Current therapeutics and practical management strategies for pulmonary arterial hypertension. Am Heart J 2011;162:201-13.
3. Liu D, Liu QQ, Eyries M, Wu WH, Yuan P, Zhang R, et al. Molecular genetics and clinical features of Chinese IPAH and HPAH patients. Eur Respir J 2012;39:597-603.
4. Dewachter L, Adnot S, Guignabert C, Tu L, Marcos E, Fadel E, et al. Bone morphogenetic protein signalling in heritable versus idiopathic pulmonary hypertension. Eur Respir J 2009;34:1100-10.
5. Austin ED, Menon S, Hemnes AR, Robinson LJ, Talati M, Fox KL, et al. Idiopathic and heritable PAH perturb common molecular pathways, correlated with increased MSX1 expression. Pulm Circ 2011;1:389-98.
6. Majka S, Hagen M, Blackwell T, Harral J, Johnson JA, Gendron R, et al. Physiologic and molecular consequences of endothelial Bmpr2 mutation. Respir Res 2011;12:84.
7. Rehman J, Archer SL. A proposed mitochondrial-metabolic mechanism for initiation and maintenance of pulmonary arterial hypertension in fawn-hooded rats: The Warburg model of pulmonary arterial hypertension. Adv Exp Med Biol 2010;661:171-85.
8. Piao L, Marsboom G, Archer SL. Mitochondrial metabolic adaptation in right ventricular hypertrophy and failure. J Mol Med (Berl) 2010;88:1011-20.
9. Sutendra G, Bonnet S, Rochefort G, Haromy A, Folmes KD, Lopaschuk GD, et al. Fatty acid oxidation and malonyl-CoA decarboxylase in the vascular remodeling of pulmonary hypertension. Sci Transl Med 2010;2:44ra58.
10. Xu W, Koeck T, Lara AR, Neumann D, DiFilippo FP, Koo M, et al. Alterations of cellular bioenergetics in pulmonary artery endothelial cells. Proc Natl Acad Sci U S A 2007;104:1342-7.
11. Fijalkowska I, Xu W, Comhair SA, Janocha AJ, Mavrakis LA, Krishnamachary B, et al. Hypoxia inducible-factor1alpha regulates the metabolic shift of pulmonary hypertensive endothelial cells. Am J Pathol 2010;176:1130-8.
12. Pugh ME, Robbins IM, Rice TW, West J, Newman JH, Hemnes AR. Unrecognized glucose intolerance is common in pulmonary arterial hypertension. J Heart Lung Transplant 2011;30:904-11.
13. Hansmann G, Wagner RA, Schellong S, Perez VA, Urashima T, Wang L, et al. Pulmonary arterial hypertension is linked to insulin resistance and reversed by peroxisome proliferator-activated receptor-gamma activation. Circulation 2007;115:1275-84.
14. Archer SL, Gomberg-Maitland M, Maitland ML, Rich S, Garcia JG, Weir EK. Mitochondrial metabolism, redox signaling, and fusion: A mitochondria-ROS-HIF-1alpha-Kv1.5 O2-sensing pathway at the intersection of pulmonary hypertension and cancer. Am J Physiol Heart Circ Physiol 2008;294:H570-8.
15. Bonnet S, Michelakis ED, Porter CJ, Andrade-Navarro MA, Thebaud B, Haromy A, et al. An abnormal mitochondrial-hypoxia inducible factor-1alpha-Kv channel pathway disrupts oxygen sensing and triggers pulmonary arterial hypertension in fawn hooded rats: similarities to human pulmonary arterial hypertension. Circulation 2006;113:2630-41.
16. McMurtry MS, Bonnet S, Wu X, Dyck JR, Haromy A, Hashimoto K, et al. Dichloroacetate prevents and reverses pulmonary hypertension by inducing pulmonary artery smooth muscle cell apoptosis. Circ Res 2004;95:830-40.
17. Michelakis ED, McMurtry MS, Wu XC, Dyck JR, Moudgil R, Hopkins TA, et al. Dichloroacetate, a metabolic modulator, prevents and reverses chronic hypoxic pulmonary hypertension in rats: Role of increased expression and activity of voltage-gated potassium channels. Circulation 2002;105:244-50.
18. Fang YH, Piao L, Hong Z, Toth PT, Marsboom G, Bache-Wiig P, et al. Therapeutic inhibition of fatty acid oxidation in right ventricular hypertrophy: Exploiting Randle's cycle. J Mol Med (Berl) 2012;90:31-43.
19. Krump-Konvalinkova V, Bittinger F, Unger RE, Peters K, Lehr HA, Kirkpatrick CJ. Generation of human pulmonary microvascular endothelial cell lines. Lab Invest 2001;81:1717-27.
20. Shen JS, Meng XL, Schiffmann R, Brady RO, Kaneski CR. Establishment and characterization of Fabry disease endothelial cells with an extended lifespan. Mol Genet Metab 2007;92:137-44.
21. Abdallah BM, Haack-Sorensen M, Burns JS, Elsnab B, Jakob F, Hokland P, et al. Maintenance of differentiation potential of human bone marrow mesenchymal stem cells immortalized by human telomerase reverse transcriptase gene despite [corrected] extensive proliferation. Biochem Biophys Res Commun 2005;326:527-38.
22. Lane KL, Talati M, Austin E, Hemnes AR, Johnson JA, Fessel JP, et al. Oxidative injury is a common consequence of BMPR2 mutations. Pulm Circ 2011;1:72-83.
23. West J, Cogan J, Geraci M, Robinson L, Newman J, Phillips JA, et al. Gene expression in BMPR2 mutation carriers with and without evidence of pulmonary arterial hypertension suggests pathways relevant to disease penetrance. BMC Med Genomics 2008;1:45.
24. Reitman ZJ, Jin G, Karoly ED, Spasojevic I, Yang J, Kinzler KW, et al. Profiling the effects of isocitrate dehydrogenase 1 and 2 mutations on the cellular metabolome. Proc Natl Acad Sci U S A 2011;108:3270-5.
25. Sreekumar A, Poisson LM, Rajendiran TM, Khan AP, Cao Q, Yu J, et al. Metabolomic profiles delineate potential role for sarcosine in prostate cancer progression. Nature 2009;457:910-4.
26. Dehaven CD, Evans AM, Dai H, Lawton KA. Organization of GC/MS and LC/MS metabolomics data into chemical libraries. J Cheminform 2010;2:9.
27. Storey JD, Tibshirani R. Statistical significance for genomewide studies. Proc Natl Acad Sci U S A 2003;100:9440-5.
28. Rudarakanchana N, Flanagan JA, Chen H, Upton PD, Machado R, Patel D, et al. Functional analysis of bone morphogenetic protein type II receptor mutations underlying primary pulmonary hypertension. Hum Mol Genet 2002;11:1517-25.
29. Foletta VC, Lim MA, Soosairajah J, Kelly AP, Stanley EG, Shannon M, et al. Direct signaling by the BMP type II receptor via the cytoskeletal regulator LIMK1. J Cell Biol 2003;162:1089-98.
30. Machado RD, Rudarakanchana N, Atkinson C, Flanagan JA, Harrison R, Morrell NW, et al. Functional interaction between BMPR-II and Tctex-1, a light chain of Dynein, is isoform-specific and disrupted by mutations underlying primary pulmonary hypertension. Hum Mol Genet 2003;12:3277-86.
31. Wong WK, Knowles JA, Morse JH. Bone morphogenetic protein receptor type II C-terminus interacts with c-Src: implication for a role in pulmonary arterial hypertension. Am J Respir Cell Mol Biol 2005;33:438-46.
32. West J, Fagan K, Steudel W, Fouty B, Lane K, Harral J, et al. Pulmonary hypertension in transgenic mice expressing a dominant-negative BMPRII gene in smooth muscle. Circ Res 2004;94:1109-14.

33. Tada Y, Majka S, Carr M, Harral J, Crona D, Kuriyama T, et al. Molecular effects of loss of BMPR2 signaling in smooth muscle in a transgenic mouse model of PAH. Am J Physiol Lung Cell Mol Physiol 2007;292:L1556-63.
34. West J, Harral J, Lane K, Deng Y, Ickes B, Crona D, et al. Mice expressing BMPR2R899X transgene in smooth muscle develop pulmonary vascular lesions. Am J Physiol Lung Cell Mol Physiol 2008;295:L744-55.
35. Vander Heiden MG, Cantley LC, Thompson CB. Understanding the Warburg effect: the metabolic requirements of cell proliferation. Science 2009;324:1029-33.
36. Reitman ZJ, Yan H. Isocitrate dehydrogenase 1 and 2 mutations in cancer: alterations at a crossroads of cellular metabolism. J Natl Cancer Inst 2010;102:932-41.
37. Tong WH, Sourbier C, Kovtunovych G, Jeong SY, Vira M, Ghosh M, et al. The glycolytic shift in fumarate-hydratase-deficient kidney cancer lowers AMPK levels, increases anabolic propensities and lowers cellular iron levels. Cancer Cell 2011;20:315-27.
38. Possemato R, Marks KM, Shaul YD, Pacold ME, Kim D, Birsoy K, et al. Functional genomics reveal that the serine synthesis pathway is essential in breast cancer. Nature 2011;476:346-50.
39. Owen OE, Kalhan SC, Hanson RW. The key role of anaplerosis and cataplerosis for citric acid cycle function. J Biol Chem 2002;277:30409-12.
40. Scott DA, Richardson AD, Filipp FV, Knutzen CA, Chiang GG, Ronai ZA, et al. Comparative metabolic flux profiling of melanoma cell lines: beyond the Warburg effect. J Biol Chem 2011;9:42626-34.
41. Shiva S, Sack MN, Greer JJ, Duranski M, Ringwood LA, Burwell L, et al. Nitrite augments tolerance to ischemia/reperfusion injury via the modulation of mitochondrial electron transfer. J Exp Med 2007;204:2089-102.
42. Dyck JR, Hopkins TA, Bonnet S, Michelakis ED, Young ME, Watanabe M, et al. Absence of malonyl coenzyme A decarboxylase in mice increases cardiac glucose oxidation and protects the heart from ischemic injury. Circulation 2006;114:1721-8.
43. Tuder RM, Davis LA, Graham BB. Targeting Energetic Metabolism: A new frontier in the pathogenesis and treatment of pulmonary hypertension. Am J Respir Crit Care Med 2012;185:260-6.
44. Yan H, Parsons DW, Jin G, McLendon R, Rasheed BA, Yuan W, et al. IDH1 and IDH2 mutations in gliomas. N Engl J Med 2009;360:765-73.
45. Kil IS, Kim SY, Lee SJ, Park JW. Small interfering RNA-mediated silencing of mitochondrial NADP+-dependent isocitrate dehydrogenase enhances the sensitivity of HeLa cells toward tumor necrosis factor-alpha and anticancer drugs. Free Radic Biol Med 2007;43:1197-207.
46. Figueroa ME, Abdel-Wahab O, Lu C, Ward PS, Patel J, Shih A, et al. Leukemic IDH1 and IDH2 mutations result in a hypermethylation phenotype, disrupt TET2 function, and impair hematopoietic differentiation. Cancer Cell 2010;18:553-67.
47. Amary MF, Bacsi K, Maggiani F, Damato S, Halai D, Berisha F, et al. IDH1 and IDH2 mutations are frequent events in central chondrosarcoma and central and periosteal chondromas but not in other mesenchymal tumours. J Pathol 2011;224:334-43.
48. Tuder RM, Chacon M, Alger L, Wang J, Taraseviciene-Stewart L, Kasahara Y, et al. Expression of angiogenesis-related molecules in plexiform lesions in severe pulmonary hypertension: evidence for a process of disordered angiogenesis. J Pathol 2001;195:367-74.
49. Raimundo N, Baysal BE, Shadel GS. Revisiting the TCA cycle: Signaling to tumor formation. Trends Mol Med 2011;17:641-9.
50. Wise DR, Ward PS, Shay JE, Cross JR, Gruber JJ, Sachdeva UM, et al. Hypoxia promotes isocitrate dehydrogenase-dependent carboxylation of alpha-ketoglutarate to citrate to support cell growth and viability. Proc Natl Acad Sci U S A 2011;108:19611-6.
51. Archer SL, Marsboom G, Kim GH, Zhang HJ, Toth PT, Svensson EC, et al. Epigenetic attenuation of mitochondrial superoxide dismutase 2 in pulmonary arterial hypertension: a basis for excessive cell proliferation and a new therapeutic target. Circulation 2010;121:2661-71.
52. Rydstrom J. Mitochondrial NADPH, transhydrogenase and disease. Biochim Biophys Acta 2006;1757:721-6.
53. Marsboom G, Wietholt C, Haney CR, Toth PT, Ryan JJ, Morrow E, et al. Lung 18F-Fluorodeoxyglucose positron emission tomography for diagnosis and monitoring of pulmonary arterial hypertension. Am J Respir Crit Care Med 2012;185:670-9.
54. Chow KS, Jun D, Helm KM, Wagner DH, Majka SM. Isolation & characterization of Hoechst(low) CD45(negative) mouse lung mesenchymal stem cells. J Vis Exp 2011:e3159.
55. Vergadi E, Chang MS, Lee C, Liang OD, Liu X, Fernandez-Gonzalez A, et al. Early macrophage recruitment and alternative activation are critical for the later development of hypoxia-induced pulmonary hypertension. Circulation 2011;123:1986-95.

SUPPLEMENTAL REFERENCES

1. Ohta T, Masutomi N, Tsutsui N, Sakairi T, Mitchell M, Milburn MV, Ryals JA, Beebe KD, Guo L. Untargeted metabolomic profiling as an evaluative tool of fenofibrate-induced toxicology in Fischer 344 male rats. *Toxicol Pathol.* 2009;37(4):521-535.
2. Evans AM, DeHaven CD, Barrett T, Mitchell M, Milgram E. Integrated, nontargeted ultrahigh performance liquid chromatography/electrospray ionization tandem mass spectrometry platform for the identification and relative quantification of the small-molecule complement of biological systems. *Anal Chem.* Aug 15 2009;81(16):6656-6667.
3. Dehaven CD, Evans AM, Dai H, Lawton KA. Organization of GC/MS and LC/MS metabolomics data into chemical libraries. *J Cheminform.* 2010;2(1):9.
4. Storey JD, Tibshirani R. Statistical significance for genomewide studies. *Proc Natl Acad Sci U S A.* Aug 5 2003;100(16):9440-9445.

Source of Support: This work was supported in part by the Vanderbilt Clinical and Translational Science Awards grant UL1 RR024975-01 from the National Center for Research Resources/NIH, by support provided to JPF by NIH training grant T32 HL094296-02, and by R01 HL095797-01A2 (JW)., **Conflict of Interest:** None declared.

SUPPLEMENTAL FIGURES

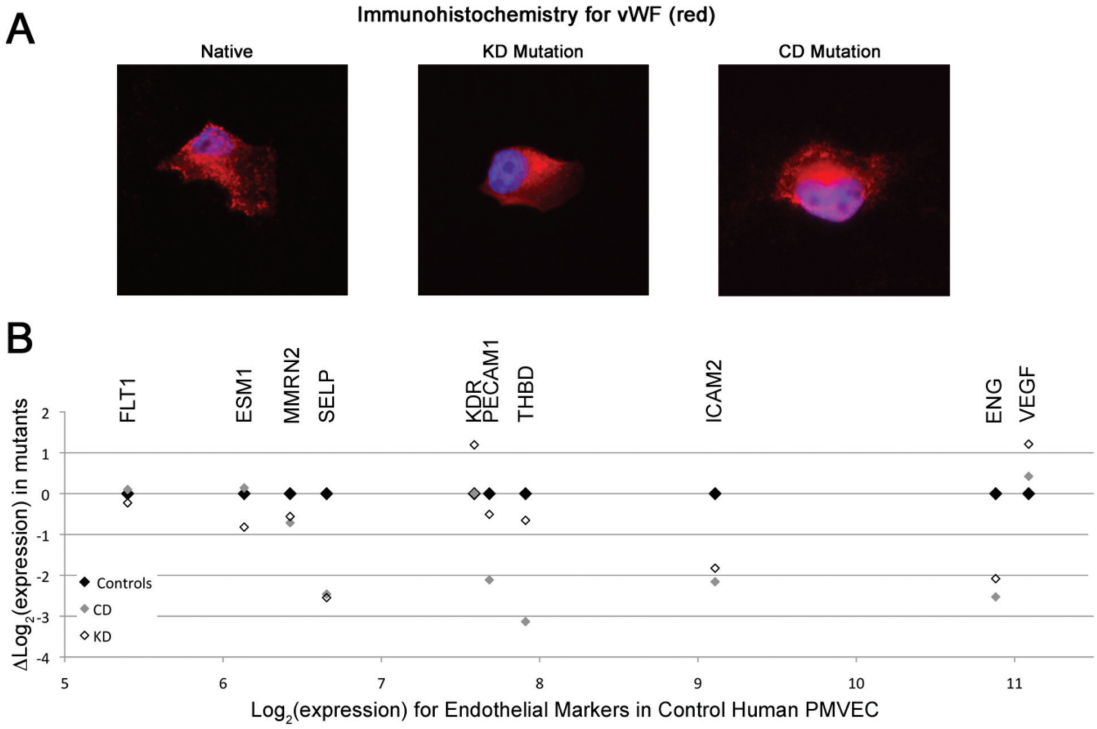

Figure S1: Native and mutant hPMVEC retain endothelial character in culture. **(A)** Immunohistochemistry for von Willebrand factor (red, with DAPI nuclear stain in blue) shows that hPMVEC retain functional expression of a canonical endothelial protein, and that expression of the mutant *BMPR2* constructs does not change this substantially. Cells shown are representative. **(B)** A panel of ten endothelial markers quantified in expression arrays shows that expression of these markers is retained in the mutant hPMVEC, confirming endothelial character. Markers are as follows: *FLT1*, vascular endothelial growth factor receptor 1; *ESM1*, endothelial cell-specific molecule 1; *MMRN2*, multimerin 2; *SELP*, selectin P; *KDR*, vascular endothelial growth factor receptor 2; *PECAM1*, platelet/endothelial cell adhesion molecule; *THBD*, thrombomodulin; *ICAM2*, intercellular adhesion molecule 2; *ENG*, endoglin; *VEGF*, vascular endothelial growth factor.

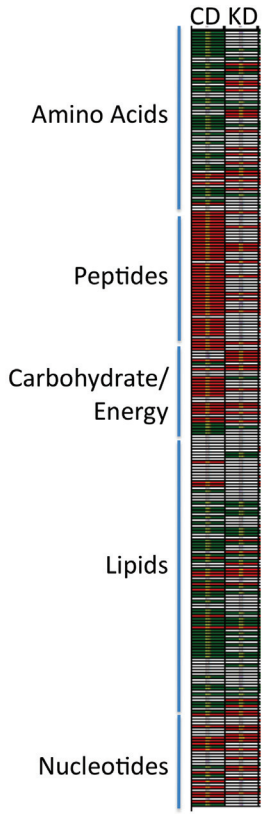

Figure S2: Overall heatmap for the metabolomic changes in CD and KD mutant hPMVEC compared to native hPMVEC. Metabolites are shown grouped by superpathway and subpathway. Data are displayed as fold change in each metabolite for each mutant relative to the native. Statistically significant changes are denoted with red for increase above the level in native hPMVEC and green for decrease below native levels.

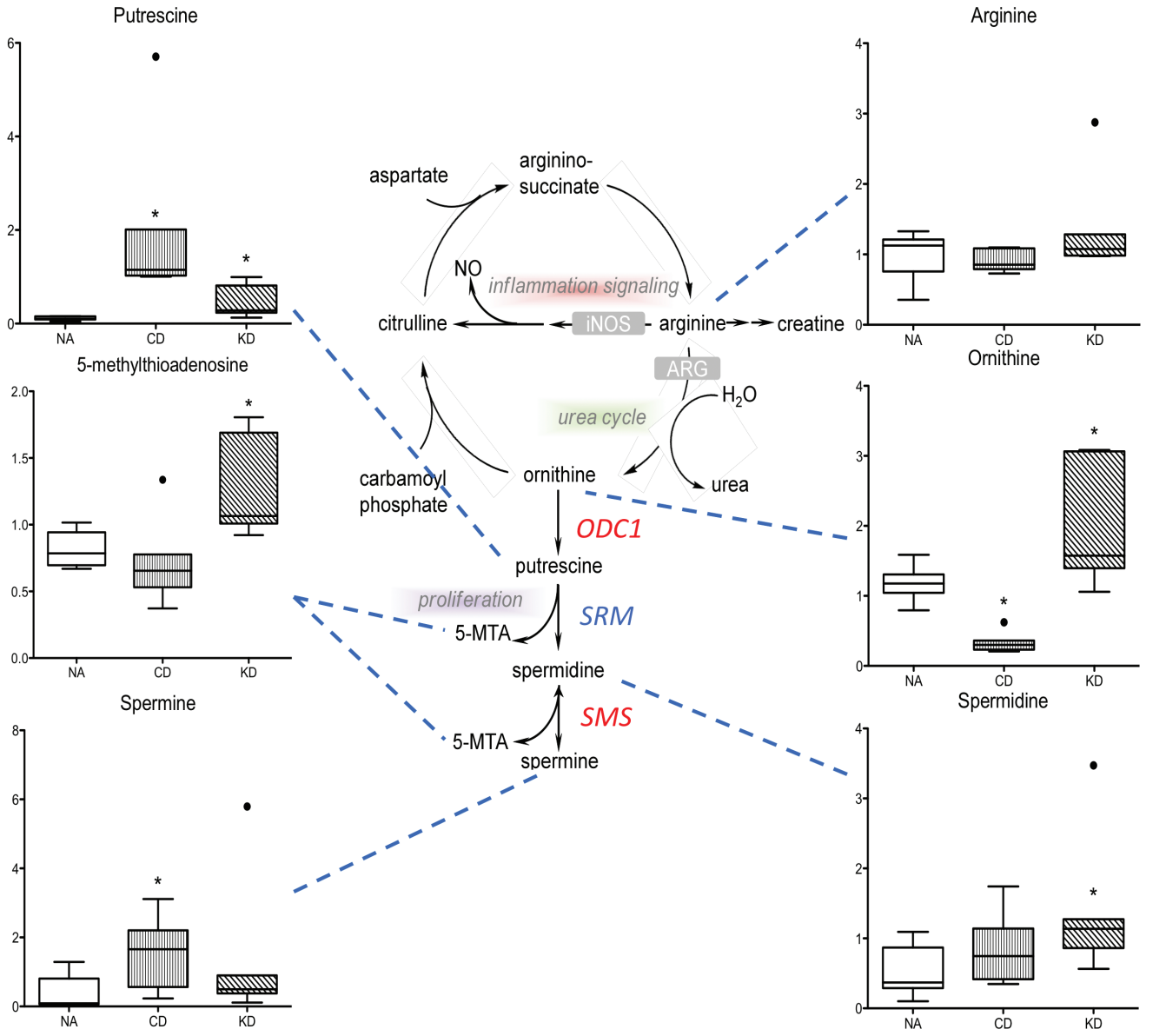

Figure S3: The polyamine biosynthetic pathway is significant upregulated in BMPR2 mutant hPMVEC. The major intermediates in the urea cycle and the polyamine biosynthetic pathway are listed. Intermediates that were confidently identified at detectable quantities are shown. In all graphs, native hPMVEC are in white boxes, CD hPMVEC in vertical hatched boxes, and KD hPMVEC in diagonal hatched boxes. Quantities are in arbitrary units specific to the internal standards for each quantified metabolite and normalized to protein concentration. N=7 for each box, with whiskers indicating Tukey whiskers and extreme data points indicated by filled circles. *P<0.05 compared to native. Genes coding for the enzymes that catalyze particular steps in the pathway are indicated by their Entrez Gene names, with red indicating significantly increased expression in the transcriptomic analysis and blue indicating significantly decreased.

Dipeptides	CD/NA	KD/NA
glycylvaline	1.44	1.49
glycylglycine	0.96	1.19
glycylproline	0.81	0.94
glycylisoleucine	1.72	1.91
glycylleucine	1.59	1.99
glycylphenylalanine	3.94	6.11
glycyltyrosine	2.79	3.48
glycyltryptophan	3.98	4.61
alanylvaline	4.43	4.63
alanylmethionine	2.22	2.57
alanylleucine	2.33	2.58
alanylisoleucine	1.88	2.15
alanylphenylalanine	2.54	3.46
alanyltyrosine	4.27	4.54
aspartylphenylalanine	3.54	4.31
aspartate-glutamate	1.82	2.61
isoleucylleucine	3.59	4.96
leucylleucine	2.93	3.92
threonylphenylalanine	2.55	2.86
phenylalanylphenylalanine	2.80	4.07
cysteinylglycine	0.70	1.45
valylleucine	3.09	3.69
arginylleucine	2.41	3.45
aspartylleucine	2.33	3.08
isoleucylalanine	2.57	2.32
isoleucylglutamate	3.90	4.50
isoleucylglutamine	3.36	3.57
isoleucylglycine	1.65	1.76
isoleucylmethionine	2.76	3.26
isoleucylserine	3.47	2.74
isoleucylvaline	3.55	3.70
leucylalanine	3.63	4.10
leucylarginine	3.56	3.49
leucylaspartate	2.81	3.55
leucylglutamate	2.53	3.09
leucylglycine	4.30	4.14
leucylphenylalanine	3.36	4.29
leucylserine	3.29	3.89
leucyltryptophan	2.38	4.25
lysylleucine	1.00	1.00
phenylalanylleucine*	2.30	2.77
phenylalanylserine	2.42	2.85
serylleucine	3.23	2.49
serylphenyalanine	2.85	2.93
threonylleucine	2.64	2.81
tryptophylleucine	2.51	3.48
tyrosylalanine	1.76	1.85
tyrosylleucine	2.95	3.93
valylisoleucine	3.51	4.50
alpha-glutamyltyrosine	2.39	3.11
leucylmethionine	2.70	3.37

Figure S4: Dipeptides are significantly increased in mutant hPMVEC. Data are displayed as fold change in each metabolite for each mutant relative to the native. Statistically significant changes are denoted with red for increase above the level in native hPMVEC.

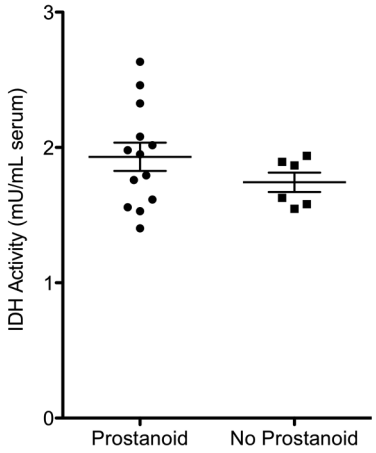

Figure S5: Serum IDH1/2 activity trends toward being higher in PAH patients on prostanoid therapy compared to PAH patients not treated with a prostacyclin receptor agonist. IDH activity measurements from heritable and idiopathic PAH patients were pooled and grouped based on prostanoid therapy status at the time of sample collection for those patients for whom such data were available. N=13 in the prostanoid group, N=6 in the no prostanoid group, mean±SEM for each group indicated, *P*=0.1 by Welch's two-sample t-test.